Solubility of carbon dioxide in aqueous piperazine solutions

Derks, P. W. J.; Dijkstra, H. B. S.; Hogendoorn, J. A.; Versteeg, G. F.

Published in:
AIChE Journal

DOI:
10.1002/aic.10442

Publication date:
2005

Solubility of Carbon Dioxide in Aqueous Piperazine Solutions

P. W. J. Derks, H. B. S. Dijkstra, J. A. Hogendoorn, and G. F. Versteeg
Dept. of Science and Technology, University of Twente, 7500 AE Enschede, The Netherlands

DOI 10.1002/aic.10442
Published online May 18, 2005 in Wiley InterScience (www.interscience.wiley.com).

In the present work, new experimental data are presented on the solubility of carbon dioxide in aqueous piperazine solutions, for concentrations of 0.2 and 0.6 molar piperazine and temperatures of 25, 40, and 70°C respectively. The present data, and other data available in the literature, were correlated using a model based on the electrolyte equation of state (EoS), as originally proposed by Fürst and Renon. The final model derived, containing only seven adjustable (ionic) parameters, was able to describe the available experimental solubility data (>150 data points for total and/or CO_2 partial pressure) with an average deviation of 16%. © 2005 American Institute of Chemical Engineers
AIChE J, 51: 2311–2327, 2005
Keywords: carbon dioxide, piperazine, solubility, electrolyte equation of state, absorption

Introduction

The selective or bulk removal of carbon dioxide from process gas streams is an important step in many industrial processes, for a number of possible reasons. In the presence of water, CO_2—which is an acid gas—can cause corrosion to process equipment. Secondly, it reduces the heating value of a natural gas stream and wastes valuable pipeline capacity. In LNG (liquefied natural gas) plants, it should be removed to prevent freezing in the low-temperature chillers, whereas it would poison the catalyst in the manufacture of ammonia. Finally, CO_2—which is also a greenhouse gas—is also held responsible for the recent climate changes. One technology used in the removal of carbon dioxide is the absorption–desorption process, in which (solutions of) alkanolamines are frequently used as solvents.[1] Depending on the process requirements, different types and combinations of (alkanolamine-based) solvents can be used.

Nowadays, the addition of an accelerator, or more specifically piperazine (PZ), to aqueous *N*-methyldiethanolamine (MDEA) solutions has found widespread application in the removal and absorption of carbon dioxide from process gases. The success of such a blend of a primary or secondary amine with a tertiary amine is based on the relatively high rate of reaction of CO_2 with the former combined with the low heat of reaction of CO_2 with the latter, which leads to higher rates of absorption in the absorber column and lower heats of regeneration in the stripper section. Crucial for an optimal design and operation of absorber and stripper is detailed knowledge concerning mass transfer and kinetics on one hand and thermodynamic equilibrium on the other hand.

The objective of this study is first to present experimental data on the CO_2 equilibrium solubility in aqueous PZ solutions, which are complementary to data already available in the literature.[2-4] More experimental data than currently available in the literature are necessary because these published data sets are restricted to low-concentration, low-pressure data on one hand and high-concentration, high-pressure on the other hand. Secondly, a thermodynamic model is described in this paper to correlate all (reliable) experimental data.

In the literature, many thermodynamic models have been presented to describe the solubilities of acid gases such as CO_2 and H_2S in (blends of) amine solutions. The applied models can be subdivided into three different approaches:

(1) The empirical approach as introduced by Kent and Eisenberg.[5]

(2) The application of an excess Gibbs energy model ("the γ–φ approach"), which forms the basis for the electrolyte

Correspondence concerning this article should be addressed to G. F. Versteeg at g.f.versteeg@utwente.nl.

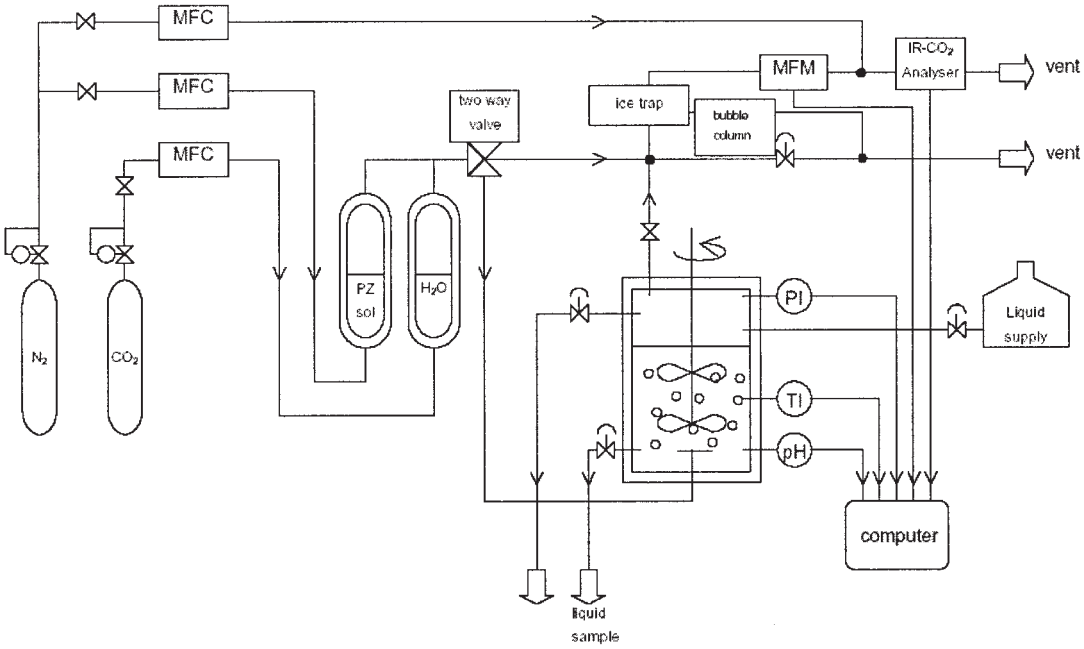

Figure 1. "Continuous" setup.

NRTL (Non-Random Two Liquid) model (for example, Austgen et al.[6]) and the Clegg–Pitzer equation (for example, Li and Mather[7]).

(3) The use of an equation of state (EoS) model, which is a fairly new development, finding application in recent publications.[8-12] Only a few papers using an EoS approach have been published so far, all but one applying the electrolyte EoS as originally proposed by Fürst and Renon.[13] Kuranov et al.[9] applied the hole theory in their EoS, but they correlated a limited set of experimental data.

In the present article, also the electrolyte EoS approach is applied, mostly based on the following considerations:

- Identical equations for gas and liquid phase
- Relatively straightforward fitting procedures of binary/ionic parameters
- Pressure effects are taken into account
- Possibility to extend the model to include hydrocarbons.

It must be noted, however, that some of the above-mentioned considerations can also be applicable to other models.

Recent publications have focused on correlating CO_2 (and H_2S) solubility and partial pressure for aqueous MDEA[10,12] and DEA[11] solutions with results comparable to those obtained with the NRTL model. Before being able to describe also the (quaternary) system MDEA–PZ–H_2O–CO_2, all (reactive) ternary subsystems need to be correlated. Therefore, this article will focus on the reactive subsystem PZ–H_2O–CO_2, presenting new data on the CO_2 solubility in aqueous piperazine solutions and correlating both these and other published experimental data sets with the electrolyte EoS.

Experimental

Experiments with diluted CO_2 using a continuous gas feed

The experimental setup and procedure are similar to those as used by Kumar et al.[14] and will therefore be described only briefly here. The setup is shown in Figure 1. For the experiments with diluted gas streams, the operation with respect to the liquid was always batchwise, whereas the mode with respect to gas phase was continuous. The heart of the setup consisted of a thermostated reactor (volume $\sim$ 1.6 L), equipped with a high-intensity gas-inducing impeller in the liquid phase and a propeller-type impeller in the gas phase. Also, the reactor was provided with a digital pressure transducer and a thermocouple. During continuous operation with respect to the gas phase, the inlet gas flows of both N_2 and CO_2 were controlled using mass flow controllers (Brooks, type 5850). Before entering the reactor, the desired gas flows of N_2 and CO_2 were presaturated with a piperazine solution identical to the one in the reactor and water, respectively. After presaturation, the gas flows were mixed and fed to the bottom of the reactor using a sintered stainless steel sparger. The outlet gas flow of the reactor was continuously analyzed for CO_2 content using an IR analyzer, type UNOR 610.

In a typical experiment, a known amount of piperazine (99%, Aldrich) was dissolved in about 500 mL of water and charged to the reactor. The mass flow controllers were adjusted to obtain the desired feed flow and composition. Next, the gas was passed through the reactor and upon attainment of equilibrium (that is, the gas inlet composition equals the outlet composition), the gas phase CO_2 content was recorded and subsequently a sample was drawn from the liquid phase. From this liquid sample both the amount of piperazine (standard potentiometric titration with 0.1 N HCl) and the total CO_2 content (desorption/titration procedure as described by Blauwhoff[15]) in the mixture were determined.

Experiments with pure CO_2 using the batch mode in the gas phase

Experimental data for CO_2 partial pressures exceeding 25 kPa were obtained in a second setup, which mainly consisted of a thermostated vigorously stirred reactor ($\sim$ 2 L) connected to

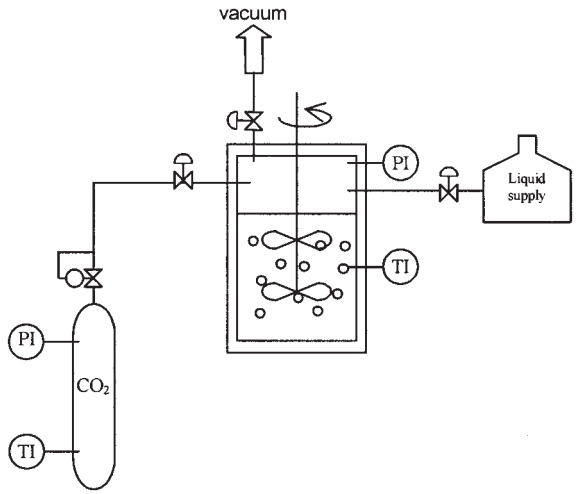

Figure 2. "Batch" setup.

a calibrated gas vessel (see Figure 2). Both reactor and gas supply vessel were equipped with a temperature and pressure indicator. Also, a vacuum pump was connected to the reactor, to remove all inert gases from the setup and dissolved gases from the amine solutions before an experiment.

In a typical experiment, a known amount of piperazine solution (prepared in the same way as described in the previous section) was transferred to the reactor vessel, after which the liquid was degassed by applying vacuum for a short while. Next, the solution was allowed to equilibrate at the desired temperature and consecutively the (vapor) pressure was recorded. Then, the gas supply vessel was filled with pure carbon dioxide and the initial pressure in this vessel was measured. Next, the stirrer was switched on and a sufficient amount of CO_2 was fed from the gas supply vessel to the reactor. The gas supply vessel to the reactor was closed and the contents of the reactor were allowed to reach equilibrium, which was reached when the reactor pressure remained constant. The actual CO_2 partial pressure could be calculated from this final (equilibrium) reactor pressure corrected for the vapor pressure of the lean solution, thereby assuming that the solution vapor pressure is not influenced by the CO_2 loading. The difference between initial and final pressure in the gas vessel was used to calculate the corresponding CO_2 loading of the solution. In some experiments, the loading was also analyzed with the technique as used during the continuous setup experiments. The actual piperazine concentration in the solutions was determined afterward using a standard potentiometric titration with 0.1 N HCl.

Experiments have been carried out for two piperazine concentrations (200 and 600 mol m^{-3}) at temperatures of 298, 313, and 343 K.

Theoretical Background

Chemical equilibrium

Because the process is chemical absorption of carbon dioxide, several chemical equilibria have to be taken into account in the modeling, considering both acid–base as well as (di)carbamate formation/hydrolysis reactions:

- Water dissociation

$$2H_2O \overset{K_I}{\rightleftharpoons} OH^- + H_3O^+$$

- Bicarbonate formation

$$2H_2O + CO_2 \overset{K_{II}}{\rightleftharpoons} HCO_3^- + H_3O^+$$

- Carbonate formation

$$H_2O + HCO_3^- \overset{K_{IIb}}{\rightleftharpoons} CO_3^{2-} + H_3O^+$$

- Piperazine protonation

$$H_2O + PZH^+ \overset{K_{III}}{\rightleftharpoons} PZ + H_3O^+$$

- Piperazine diprotonation

$$H_2O + PZH_2^{2+} \overset{K_{IIIb}}{\rightleftharpoons} PZH^+ + H_3O^+$$

- Hydrolysis of piperazine monocarbamate

$$PZ + HCO_3^- \overset{K_{IV}}{\rightleftharpoons} H_2O + PZCOO^-$$

- Hydrolysis of piperazine dicarbamate

$$PZCOO^- + HCO_3^- \overset{K_V}{\rightleftharpoons} H_2O + PZ(COO^-)_2$$

- Monocarbamate protonation

$$H_2O + {}^+HPZCOO^- \overset{K_{VI}}{\rightleftharpoons} PZCOO^- + H_3O^+$$

All equilibria involving carbamated piperazine species (K_{IV}, K_V, and K_{VI}) have been identified and quantified by Bishnoi and Rochelle[2] and Ermatchkov et al.[16] The equilibrium constants of the latter have been used in the present work (see Table 1) because they have been measured over a larger temperature interval.

To reduce the number of species in the model, three assumptions have been made:

(1) The first one concerns the concentration of the carbonate

Table 1. Coefficients for the Chemical Equilibrium Constants Used in the Model

	C_0	C_1	C_2	C_3	$K_{(T=313\ K)}$	T (°C)	Source
K_I	132.899	−13445.9	−22.4773	0	9.3×10^{-18}	0–225	17
K_{II}	231.465	−12092.1	−36.7816	0	9.0×10^{-9}	0–225	17
K_{IIb}	216.049	−12431.7	−35.4819	0	1.1×10^{-12}	0–225	17
K_{III}	18.135	3814.4	0	−0.015096	1.3×10^{11}	0–50	18*
K_{IIIb}	14.134	2192.3	0	−0.017396	6.5×10^{6}	0–50	18*
K_{IV}	−4.6185	3616.1	0	0	1.0×10^{3}	0–60	16*
K_V	0.36150	1322.3	0	0	98.1	0–60	16*
K_{VI}	14.042	3443.1	0	0	8.8×10^{10}	0–60	16*

*The original coefficients have been converted from the molality scale.

ion, which is assumed to be negligible, considering the pH range of interest and the equilibrium constant for this reaction (see also Table 1). The same assumption was made by Solbraa[12] and Chunxi and Fürst.[10]

(2) Secondly, it is common to neglect the mole fractions of both OH^- and H_3O^+ in the modeling of acid gas equilibria in for example, MDEA solutions[10,12] and, partially, this has also been assumed in the present work. This assumption can be justified by the fact that, on the one hand, amines such as piperazine are weak bases; on the other hand, acid gases such as CO_2 are weak acids in water. In the current model, only the H_3O^+ fraction has been neglected; because PZ is a stronger base than MDEA, the OH^- fraction does play a minor role (only at low carbon dioxide loading). The neglecting of H_3O^+ ions has been validated in initial model simulations; its fraction never exceeded the value 10^{-7}.

(3) The third simplification involves the neglecting of diprotonated piperazine (PZH_2^{2+}). This assumption is based on the second pK_a of piperazine, which is 5.3 at 298 K and thus too low to be of relevance in the current model and the pH range of interest for CO_2 removal processes.[2]

With these assumptions, the model is reduced to a system of nine species [H_2O, OH^-, CO_2, HCO_3^-, PZ, PZH^+, $PZCOO^-$, $PZ(COO^-)_2$, and $^+HPZCOO^-$], to be solved with five independent equilibrium constants, the total mass balance, total piperazine and carbon dioxide balances, and the electroneutrality condition.

All chemical equilibrium constants in this work are defined in the mole fraction scale with infinite dilution in water as the reference state for all species (except water). Mathematically, all constants are then defined as follows

$$K_{eq} = \prod_i (x_i \gamma_i)^{\nu_i} \tag{1}$$

where ν_i is the stoichiometric constant, as defined by the reactions described earlier.

The following temperature dependency is adopted for all constants

$$\ln K = C_0 + \frac{C_1}{T} + C_2 \ln T + C_3 T \tag{2}$$

Values and sources for coefficients C_0–C_3 are listed in Table 1.

The present EoS model derives each component's activity coefficient (γ_i in Eq. 1) from its fugacity coefficient φ_i, in accordance with its reference state. For water (reference state is the pure component) this implies

$$\gamma_{H_2O} = \frac{\varphi_{H_2O}(T, P, x_i)}{\varphi_{H_2O}^{pure}(T, P)} \tag{3}$$

For all other species, with reference state the infinite dilution in water, the following equation applies

$$\gamma_i = \frac{\varphi_i(T, P, x_i)}{\varphi_i(T, P, x_i \rightarrow 0)} \tag{4}$$

Equilibrium between liquid and vapor phases is attained by obeying the equal fugacity condition, as defined by the following equation

$$x_i \varphi_i^L P = f_i^L \equiv f_i^V = y_i \varphi_i^V P \tag{5}$$

The fugacity coefficient can be deduced from the residual Helmholtz energy, as shown by Eq. 6

$$RT \ln \varphi_i = \left(\frac{\partial}{\partial n_i} A^R(T, V, n)\right)_{T,P,n_{j\neq i}} - RT \ln Z \tag{6}$$

All the individual terms of the applied Helmholtz function (A^R), accounting for the system's nonideality, will be discussed in the next section.

Electrolyte equation of state

As stated in the introduction, the presently developed model is based on the electrolyte equation of state, as proposed by Fürst and Renon.[13] The general equation defines the Helmholtz energy as a sum of four contributions

$$\left(\frac{A - A^{IG}}{RT}\right) = \left(\frac{A^R}{RT}\right) = \left(\frac{A^R}{RT}\right)_{RF} + \left(\frac{A^R}{RT}\right)_{SR1} + \left(\frac{A^R}{RT}\right)_{SR2} + \left(\frac{A^R}{RT}\right)_{LR} \tag{7}$$

The first two terms take into account the energy stemming from repulsive forces (*RF*) and (attractive) short-range interactions

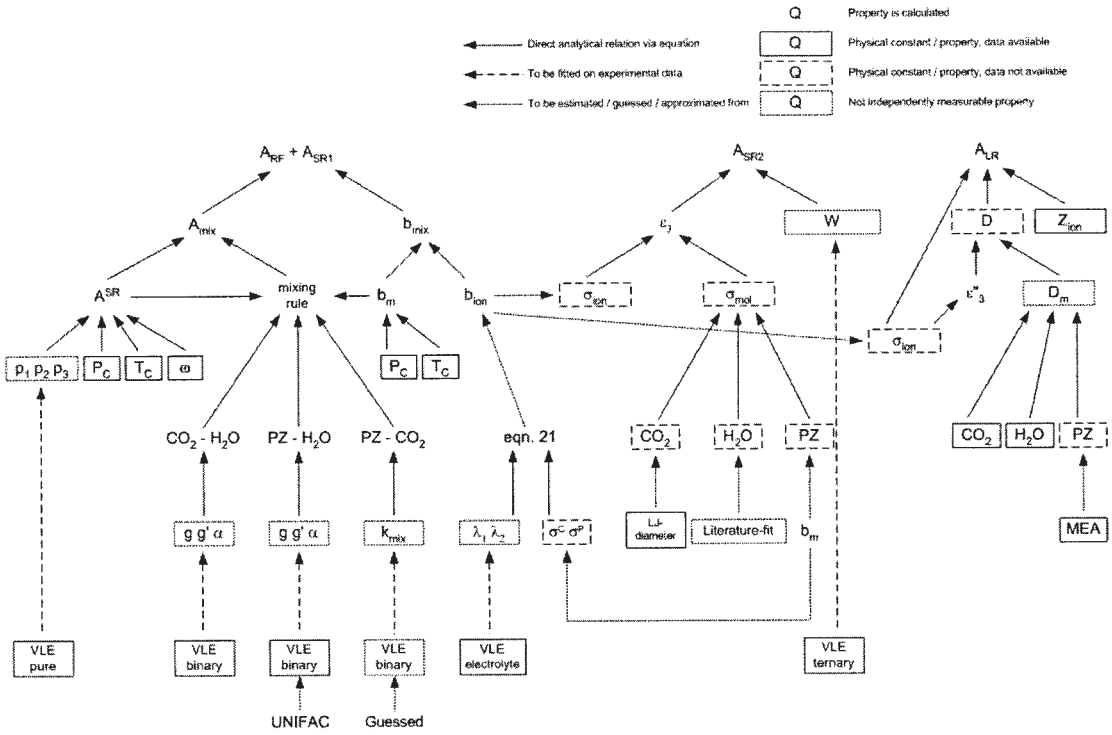

Figure 3. Overview of thermodynamic model applied.

(*SR*1), and they are implemented by means of the Redlich–Kwong–Soave (RKS) equation of state, expressed as

$$P = \frac{RT}{V - b_{mix}} - \frac{A^{SR}_{mix}}{V(V + b_{mix})} \tag{8}$$

where the presence of ions is included in the mixture covolume b_{mix}

$$b_{mix} = \sum_m x_m b_m + \sum_{ion} x_{ion} b_{ion} \qquad b_m = \frac{2^{1/3} - 1}{3} \frac{RT_C}{P_C} \tag{9}$$

The mixture attraction parameter A^{SR}_{mix} is calculated using the Huron–Vidal mixing rule[19]

$$A^{SR}_{mix} = b_{mix} \left[\sum_m \left(\frac{x_m A^{SR}_m}{b_m} \right) - \frac{G^E_\infty}{\ln 2} \right]$$

$$\frac{G^E_\infty}{RT} = \sum_m x_m \frac{\sum_n \tau_{nm} b_n x_n \exp(-\alpha_{nm}\tau_{nm})}{\sum_m b_{n'} x_{n'} \exp(-\alpha_{n'm}\tau_{n'm})}$$

$$\tau_{nm} = \frac{g_{nm} - g_{mm}}{RT}$$

$$g_{nm} - g_{mm} = (g'_{nm} - g'_{mm}) + (g''_{nm} - g''_{mm})T = \Delta g'_{nm} + \Delta g''_{nm} T \tag{10}$$

with pure components attraction parameters stemming from the expression proposed by Schwartzentruber and Renon[20]

$$A^{SR}_m = \frac{1}{9(2^{1/3} - 1)} \frac{(RT_C)^2}{P_C} \alpha(T_R) \tag{11}$$

where

$$\alpha(T_R) = [1 + m(\omega)(1 - T_R^{1/2}) - p_1(1 - T_R)(1 + p_2 T_R + p_3 T_R^2)]^2$$

and $m(\omega) = 0.48508 + 1.55191\omega - 0.1561\omega^2$.

The Helmholtz energy arising from interactions between molecules and ions and between cations and anions (*SR*2) is included in the third term, which can be regarded as the solvation contribution

$$\left(\frac{A^R}{RT} \right)_{SR2} = \sum_k \sum_l \frac{x_k x_l W_{kl}}{V(1 - \varepsilon_3)} \tag{12}$$

Table 2. List of Physical Properties and Constants of Molecular Components

Molecular Property		CO_2	H_2O	PZ	Location
Critical constants	T_c; P_c; ω	Yes*	Yes*	Yes*	Table 5
Molecular diameter	σ_m	No	No	No	Table 5
Dielectric constant	D	Yes	Yes	No	Table 5

*Availability of value of specific parameter in the open literature.

Table 3. List of Physical Properties and Constants of Ionic Species

Ionic Property		Available	Location
Charge	Z	Yes	—
Solvated diameter	σ^P; σ^C	No	Table 7
Ionic diameter	σ_{ion}	No	Eq. 22

where at least one of k and l is an ion, and ε_3 denotes the packing factor

$$\varepsilon_3 = \frac{N_A \pi}{6} \sum_k \frac{x_k \sigma_k^3}{V} \tag{13}$$

where the summation is over all species present in the solvent.

The long-range ionic forces (*LR*) are represented by a simplified mean spherical approximation (MSA) term, as proposed by Ball et al.[21]

$$\left(\frac{A^R}{RT}\right)_{LR} = -\frac{\alpha_{LR}^2}{4\pi} \sum_{ion} \frac{x_i Z_{ion}^2 \Gamma}{1 + \Gamma \sigma_{ion}} + \frac{\Gamma^3 V}{3\pi N_A} \tag{14}$$

with the shielding parameter Γ, the parameter α_{LR}, and the system's dielectric constant D, defined as follows

$$4\Gamma^2 = \alpha_{LR}^2 \sum_{ion} \frac{x_{ion}}{V} \left(\frac{Z_{ion}}{1 + \sigma_{ion}\Gamma}\right)$$

$$\alpha_{LR}^2 = \frac{e^2 N_A}{\varepsilon_0 DRT}$$

$$D = 1 + (D_S - 1)\frac{1 - \varepsilon_3''}{1 - \frac{\varepsilon_3''}{2}}$$

$$D_S = \frac{\sum_m x_m D_m}{\sum_m x_m} \tag{15}$$

where ε_3'' is calculated similarly to ε_3, although now the summation is over the ionic species only. The influence of ions on the dielectric constant is incorporated by Pottel's expression.[22]

The buildup of the Helmholtz free energy, described in Eqs. 7–15, is illustrated schematically in Figure 3 to provide an overview of all parameters and properties needed in the EoS model and their relations.

Analysis of the different kinds of parameters needed for model calculations shows that a distinction should be made between component properties and constants, on one hand, and (interaction) parameters related to the thermodynamic model applied, on the other hand.

The first group contains physical properties and/or constants that can be measured independently, such as critical temperatures and pressures and molecular and ionic diameters. Values for some of these properties, however, are not presently available in the open literature. Therefore, in some cases, an estimation of these parameters is necessary. Lists of all needed properties, their availability in the literature, and the location of the value used in the present work are given in Table 2 (molecular properties) and Table 3 (ionic properties).

The second series consists of parameters that are not independently measurable; they are a consequence of the thermodynamic relations present in the model. These parameters—with the exception of the binary parameter k_{mix} describing the binary interaction between CO_2 and PZ, which is guessed—have been determined by means of fitting the model to (pseudo-) experimental data. A list of these parameters is given in Table 4.

In the following sections, all individual properties and (fit) parameters (and their sources and/or approximation methods used) will be described in more detail.

Pure component parameters

As can be seen from Eqs. 11 and 15 several pure component parameters and properties (with respect to the attraction parameter A^{SR} or the dielectric constant D_m) need to be known before the model can be used. The first step involves the determination of the polar parameters p_1, p_2, and p_3, which are present in Schwartzentruber's expression for the pure component attraction parameter A^{SR} (Eq. 11). They were obtained by fitting them to experimental vapor pressures of pure components using the following minimization function

$$F = \sum_{exp} \left| \frac{P^{exp} - P^{mod}}{P^{exp}} \right| \tag{16}$$

Results of this fitting procedure are listed in Table 5, along with each component's critical constants.

Table 4. List of Parameters That Cannot Be Determined Independently

System	Component(s)	Parameter	Exp. Data*	Approx.	Location
Pure	CO_2	p_1, p_2, p_3	Yes	—	Table 5
	H_2O	p_1, p_2, p_3	Yes	—	Table 5
	PZ	p_1, p_2, p_3	Yes	—	Table 5
Binary	CO_2–H_2O	$\Delta g'_{nm}$, $\Delta g''_{nm}$, $\Delta g'_{mn}$, $\Delta g''_{mn}$, α	Yes	—	Table 6
	H_2O–PZ	$\Delta g'_{nm}$, $\Delta g''_{nm}$, $\Delta g'_{mn}$, $\Delta g''_{mn}$, α	No	UNIFAC	Table 6
	CO_2–PZ	k_{mix}	No	Guessed	Table 6
Electrolyte	H_2O–halide salts	λ_1, λ_2	Yes	—	Inline text
Ternary	CO_2–PZ–H_2O	$7W$	Yes	—	Table 11

*Availability of experimental data necessary for obtaining specific parameter.

Table 5. All Pure Component Parameters and Their Sources

	H_2O	PZ	CO_2
T_C (K)	647.3	661	304.2
P_C (bar)	220.9	58.0	73.8
ω	0.344	0.31	0.225
Source	23	24	23
p_1	0.074168	−0.19842	0.054244
p_2	−0.94308	−2.857	−1.2603
p_3	−0.70403	2.0373	−0.031337
Source*	25	24, 26	25, 27
d_0	−19.29	148.9	0.79062
d_1	2.98×10^4	0	0
d_2	−0.0196	−0.62491	0.010639
d_3	1.31×10^{-4}	0.771×10^{-3}	-2.851×10^{-5}
d_4	-3.11×10^{-7}	0	0
Source	10	25	25
σ (10^{-10} m)	2.52	3.96	3.94
Source	21	Eq. 18	23

*The references contain the vapor–liquid data used in the regression of parameters p_1, p_2, and p_3.

Further, the calculation of the mixture dielectric constant requires the knowledge of the dielectric constants for the pure components (see Eq. 15). In accordance with the literature, these constants were assumed to have the following temperature dependency

$$D_m = d_0 + \frac{d_1}{T} + d_2T + d_3T^2 + d_4T^3 \tag{17}$$

The values for water and carbon dioxide were derived by Chunxi and Fürst,[10] from experimental data of Akhadov[28] and Lide.[25] As in the work of Bishnoi and Rochelle,[29] the dielectric constant of piperazine was assumed to be the same as for MEA. This is allowed because the sensitivity of the model for this property is very low, which is a consequence of the relatively small fraction of molecular piperazine present in the mixtures: calculated equilibrium pressures (P_{CO_2}) changed at maximum 1.5% when decreasing the dielectric constant by a factor of 4. Constants d_0–d_4 for MEA were taken from Lide.[25] All coefficients needed to calculate D_m are listed in Table 5.

Finally, each species' molecular diameter (σ_m) is required in the determination of the packing factor. For water and carbon dioxide, these diameters are taken from the literature—the former was estimated by Ball et al.[21] and for the latter the Lennard–Jones diameter as given by Poling et al.[23] was used. For piperazine, the diameter was estimated using its covolume[10,12]

$$\sigma_{PZ} = \sigma_{H_2O}\left(\frac{b_{PZ}}{b_{H_2O}}\right)^{1/3} \tag{18}$$

Values and sources are listed in Table 5.

Table 7. Estimated Solvated Diameters for Piperazine-Related Species

	Species				
	PZ	$PZCOO^-$	$PZ(COO^-)_2$	$^+HPZCOO^-$	PZH^+
Solv. diameter (Å)	3.96	5.5	7.0	5.4	3.9

Binary interaction parameters

Because the mixture contains polar components, in this work the Huron–Vidal mixing rule was implemented to calculate the mixture attraction parameter A_{mix}^{SR}. Per binary pair, this mixing rule includes one non-randomness parameter (α_{nm}) and two interaction coefficient terms (τ_{nm} and τ_{mn}), which are temperature dependent (see Eq. 10), resulting in a total of five parameters to be derived per binary pair: $\Delta g'_{nm}$ and $\Delta g''_{nm}$, $\Delta g'_{mn}$, $\Delta g''_{mn}$, and α. For H_2O–CO_2 these parameters can be derived from experimental CO_2 gas solubility data in water at various temperatures and pressures, thereby applying the following objective function

$$F = \min \sum_{exp} \left| \frac{P_{CO_2}^{exp} - P_{CO_2}^{mod}}{P_{CO_2}^{exp}} \right| \tag{19}$$

Unfortunately, there are no (useful) binary (VLE) data for systems with PZ available in the literature. A possibility is to fit the parameters describing both PZ–H_2O and PZ–CO_2 interactions on the total (reactive) system, but—considering that this involves ten (extra) fit parameters—this could lead to erroneous results. Therefore, to reduce the number of fit parameters as well as the risk of erroneous fitting, another approach was adopted in this work.

First, the interaction parameters describing the PZ–H_2O binary system were fitted to pseudo-data, which were acquired using the Dortmund-modified UNIFAC package in Aspen Plus 11.1. Using the same goal function as that for CO_2–H_2O, the results as given in Table 6 were obtained.

Secondly, similar to the work of Solbraa,[12] the following correlations were used to describe the interaction between CO_2 and the used amine (in the present work piperazine)

$$\alpha,\ g'_{mn},\ g'_{nm} = 0$$

$$g_{mm} = -\frac{A_m^{SR}}{b_m}$$

$$g_{nm} = -2\frac{\sqrt{b_n b_m}}{b_n + b_m}(g_{nn} \cdot g_{mm})^{1/2}(1 - k_{mix}) \tag{20}$$

Table 6. Binary Interaction Coefficients Used in the Model

System	$\Delta g'_{nm}$ (kJ mol^{-1})	$\Delta g''_{nm}$ (J mol^{-1} K^{-1})	$\Delta g'_{mn}$ (kJ mol^{-1})	$\Delta g''_{mn}$ (J mol^{-1} K^{-1})	α	Reference
H_2O–CO_2	−17.76	−27.84	46.89	1.05	0.035	30*
H_2O–PZ	−9.04	31.69	−15.87	53.49	0.361	UNIFAC
CO_2–PZ		$k_{mix} = 0.2$			0	Guessed**

* The reference contains the experimental data on CO_2 solubility in H_2O used in the regression.
**The value for k_{mix} is an arbitrary one. This is allowed because the model is not sensitive to this parameter.

Table 8. Experimental VLE Data of CO_2 in 0.6 M PZ Solution

T = 25°C		T = 40°C		T = 70°C	
Loading (mol CO_2/mol PZ)	P_{CO_2} (kPa)	Loading (mol CO_2/mol PZ)	P_{CO_2} (kPa)	Loading (mol CO_2/mol PZ)	P_{CO_2} (kPa)
0.70	0.31	0.64	0.37	0.36	0.27
0.75	0.41	0.73	0.82	0.50	0.67
0.81	0.72	0.76	1.62	0.54	1.72
0.88	1.53	0.78	3.27	0.62	3.19
0.89	2.95	0.83	4.09	0.62	3.86
0.97	5.36	0.87	5.99	0.71	4.53
0.98	7.38	0.91	10.08	0.68	5.34
0.98	10.92	0.94	10.41	0.71	7.31
1.02	26.87	0.99	26.52	0.76	10.41
1.03	66.98	0.98	39.61	0.88	38.01
1.06	103.93	1.03	92.81	0.92	82.07
1.08	111.37	1.03	104.70	0.96	94.1

With these parameters, the Huron–Vidal mixing rule is reduced to the classical van der Waals mixing rule, thereby reducing the number of fitting parameters to one for the CO_2–PZ binary pair (that is, k_{mix}). Following this procedure, the number of fitting parameters for both binary systems with PZ (H_2O–PZ and CO_2–PZ) was reduced from ten to six.

All binary interaction coefficients thus obtained and used in the present model are listed in Table 6.

Ionic interaction parameters

Basically, there are three types of ionic parameters in the model: the ionic diameter σ_{ion}, the ionic covolume b_{ion}, and the ionic interaction parameters W_{kl}. To obtain reasonable estimates for both b_{ion} and σ_{ion}, the following procedure was followed:

The ionic covolume b_{ion} and the ionic diameter σ_{ion} can be calculated using the following equations[13,31]

$$b_c = \lambda_1(\sigma_c^S)^3 + \lambda_2 \qquad b_a = \lambda_1(\sigma_a^P)^3 + \lambda_2 \tag{21}$$

$$\sigma_{ion} = \sqrt[3]{\frac{6b_{ion}}{N_A\pi}} \tag{22}$$

The advantage of using Eqs. 21 and 22 is the immediate reduction in the number of unknown physical parameters from two (covolume and radius) to only one, that is, the Stokes' or Pauling solvated diameter (σ^S and σ^P). The required parameters, λ_1 and λ_2, are to be obtained by fitting VLE data of strong electrolytes (in the relevant solvent).

Solvated diameters of typical ions, such as OH^- (3.52 Å) and HCO_3^- (3.36 Å), can be found in the literature. If this is not the case (such as for $PZCOO^-$) there are two alternatives:

(1) using these parameters as adjustable (fit) parameters;

(2) making an educated guess, based on its molecular structure and the structure and diameter of the "parent molecule."

The latter procedure has been followed in this work; diameters of all piperazine-related species were determined in a manner similar to the one Vallée et al.[11] applied to obtain diameters of DEA-related species. The obtained solvated diameters are listed in Table 7.

The solvent-dependent parameters λ_1 and λ_2 were obtained by fitting the experimental osmotic data of Robinson and Stokes[32] on 28 strong electrolytes (halide salts) in water, which is the solvent in the PZ–H_2O–CO_2 systems, applying the following objective function

$$F = \min \sum_{exp} \left| \frac{\Phi^{exp} - \Phi^{mod}}{\Phi^{exp}} \right| \tag{23}$$

where Φ denotes the osmotic coefficient.

Their values were found to be $\lambda_1 = 11.27\cdot \times 10^{-7}$ m^3 mol^{-1} Å^{-3} and $\lambda_2 = 5.42\cdot \times 10^{-5}$ m^3 mol^{-1}.

As in previous work on the application of the electrolyte EoS (for example, Fürst and Renon[13]), it seems reasonable to take into account only the interactions between cations and molecules (W_{cm}) and cations and anions (W_{ca}). Other interactions were ignored because of the charge repulsion effect (anion–anion and cation–cation interaction), or because of the gener-

Table 9. Experimental VLE Data of CO_2 in 0.2 M PZ Solution

T = 25°C		T = 40°C		T = 70°C	
Loading (mol CO_2/mol PZ)	P_{CO_2} (kPa)	Loading (mol CO_2/mol PZ)	P_{CO_2} (kPa)	Loading (mol CO_2/mol PZ)	P_{CO_2} (kPa)
0.81	0.45	0.63	0.38	0.47	0.51
0.84	0.64	0.76	0.88	0.59	1.18
0.89	1.00	0.88	2.63	0.70	2.57
0.92	1.70	0.98	10.11	0.78	5.03
0.94	2.94	1.07	68.51	0.97	45.3
0.99	5.38	1.14	101.71	1.03	80.50
0.98	8.50			1.03	87.8
1.02	10.67				
1.23	107.23				

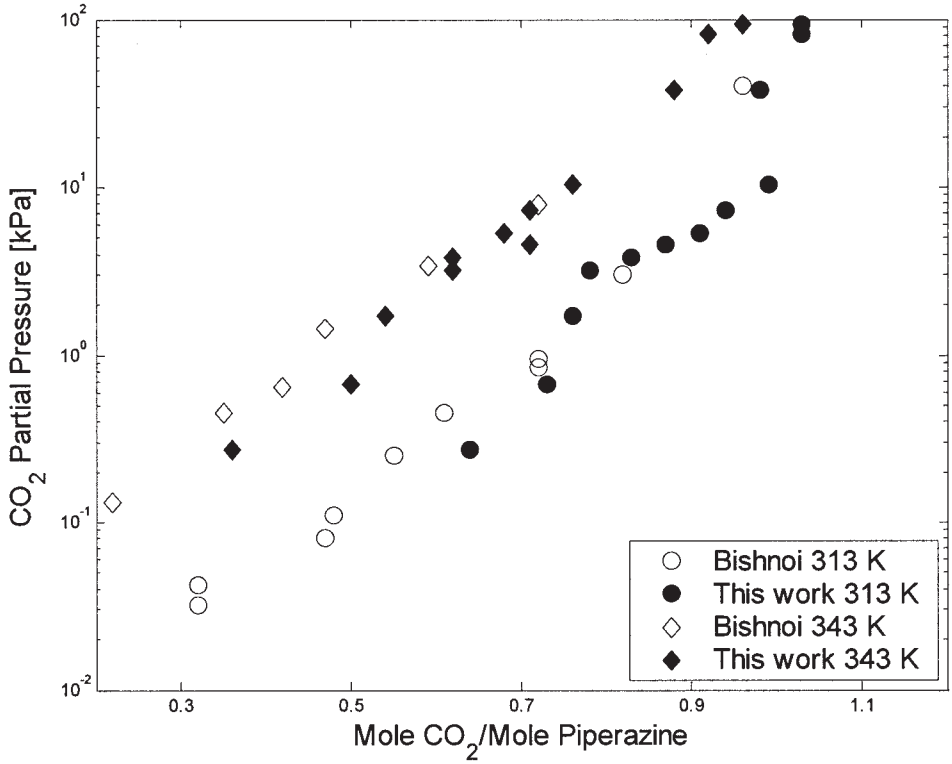

Figure 4. Comparison of the 0.6 M PZ data of Bishnoi and Rochelle[2] at 313 and 343 K with the present data.

ally lower solvation of anions compared to that of cations (anion–molecule interaction).

For the application in treating processes, the value of the OH^- mole fraction is $<10^{-6}$, which renders the influence of the interaction between OH^- and PZH^+ on the model negligible.

In total, this leaves the following seven (ionic) variables to be fitted to experimental data sets:

Cation–Molecule Interactions W_{cm}:

PZH^+ with H_2O, PZ, and CO_2

Cation–Anion/Zwitterion Interactions W_{ca}:

PZH^+ with $PZCOO^-$, $PZ(COO^-)_2$, HCO_3^-, and $^+HPZCOO^-$.

At this point, the ionic interaction coefficients W_{cm} and W_{ca} were the only unknown variables left in the set of equations needed to calculate CO_2 partial pressures with the EoS model. In the present work, they were assumed to be temperature independent. Generally, however, this assumption holds for only a limited temperature interval, as shown by Zuo and Fürst.[31]

In conclusion, a total number of seven ionic interaction coefficients W_{kl} remains, which cannot be determined independently. Therefore these parameters had to be fitted on the available VLE data, the results of which will be described in the modeling results section.

Results

Experimental results

All experimentally obtained data on CO_2 solubility with their corresponding partial pressure are listed in Tables 8 and 9 and are graphically represented in Figures 4 and 5. The experimental error in this work is estimated (based on propagation of error) at 4% in loading and 5% in CO_2 partial pressure, respectively.

When comparing the present data to those three sets already available in the literature, the following observations can be made:

(1) The solubility data in 0.6 kmol m^{-3} aqueous PZ solutions (Table 5) are in good agreement with the data presented by Bishnoi and Rochelle,[2] which is clearly illustrated in Figure 4.

(2) Aroua and Mohd Salleh[4] published CO_2 solubility data at lower piperazine concentrations—varying between 0.1 and 1.0 kmol m^{-3}—at temperatures ranging from 20 to 50°C. Because they also performed experiments with solutions containing both 0.2 and 0.6 kmol m^{-3} at a temperature of 40°C, their results are easily comparable to the current data sets but also to some data by Bishnoi.[2] This comparison is shown graphically in Figures 5a and 5b, from which it can be observed that there is a substantial (more or less constant) discrepancy between the data by Aroua[4] and the other data (Bishnoi's work[2] and this work). The large deviation of Aroua's VLE data on one hand and the current data and Bishnoi's data on the other hand seems to point out that it is useless to fit the ionic interaction parameters W_{kl} on all three experimental data sets

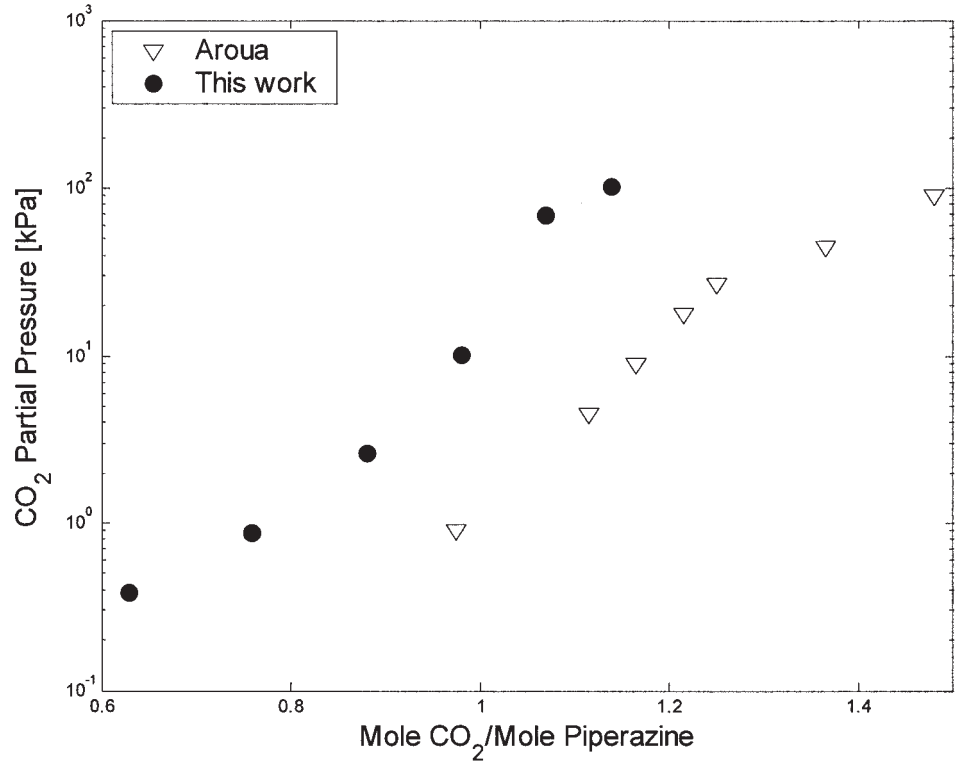

(a)

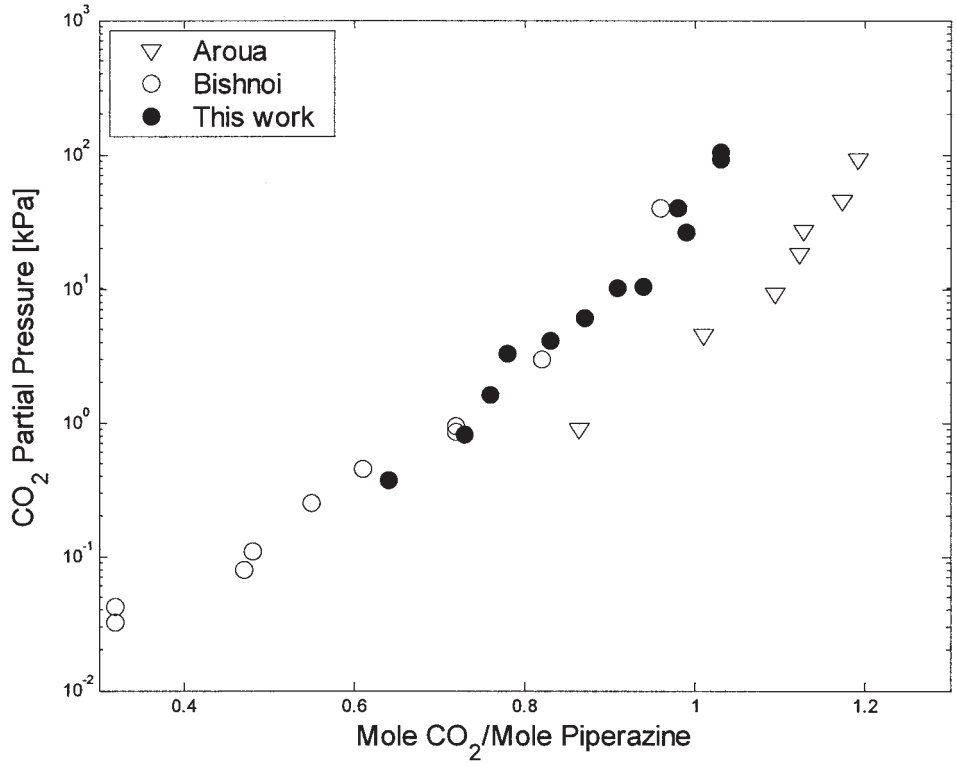

(b)

Figure 5. (a) Comparison of 0.2 M PZ data of Aroua and Mohd Salleh[4] at 313 K with the present data; (b) comparison of 0.6 M PZ data of Aroua and Mohd Salleh[4] at 313 K with the present data and data by Bishnoi and Rochelle.[2]

Table 10. Results of the Consistency Check of the Present Data at Two Different CO_2 Loadings

[PZ]	CO_2 Loading [1]	P_{CO_2} (kPa)	CO_2 Loading [2]	P_{CO_2} ($\times 10^2$ kPa)	Source
0.2 M	0.76	0.88	1.07	0.69	This work
0.6 M	0.76	1.62	1.03	0.93–1.05	This work
2.0 mol kg^{-1}	0.73	≈6	1.02	≈1.6	3*

*Pérez-Salado Kamps et al.[3] list total pressure data in their article. The values in the table are estimated by subtracting the water vapor pressure, which is 73.8 mbar at 313.15 K, from the total pressure values of 133 mbar and 1.71 bar, respectively.

simultaneously as this would result in model predictions that would deviate substantially from all three experimental data sets. As the data of Bishnoi's study seem to be consistent with the experimental data from this study, these data sets are thought to be more reliable and, therefore, only the data of Bishnoi and the experimental data as obtained in this study were used in the modeling part of this work.

(3) A thorough consistency check of the current data with the data by Pérez-Salado Kamps et al.[3] is not possible because they performed experiments in 2.0 and 4.0 molal PZ solutions. A rough consistency check, however, is possible throughout: at fixed loading and temperature, the CO_2 partial pressure should increase with increasing piperazine concentration.[10] In Table 10, experimental equilibrium pressures for three different concentrations are compared at similar loadings at a temperature of 313 K.

As shown in Table 10, the simple consistency check with the data by Pérez-Salado Kamps[3] holds. However, some low-pressure data in 2.0 molal solutions are required for a more sound comparison.

Modeling results

As mentioned earlier, the data presented by Aroua and Mohd Salleh[4] were excluded from the database used in the determination of the ionic interaction parameters W_{kl}. The database was further screened for unreliable data (series) using the two following generally found trends in acid gas VLE diagrams[10]:

(1) At a fixed loading and temperature, the CO_2 partial pressure will increase with increasing amine concentration.

(2) At a fixed loading and amine concentration, the CO_2 partial pressure will increase with increasing temperature.

In addition, initial model simulations were performed to further screen and optimize the database. When an individual experimental result and the preliminary model calculation deviated by a factor of >2, that particular data point was excluded from the database to prevent it from dominating the fit. This was the case for some data measured in the loading range around 1 (mol CO_2/mol PZ), where a steep slope exists between log P and loading. The final database consisted of 153 experimental data points (out of 170) to be used in the determination of the seven model variables W_{kl}.

To maintain consistency throughout this study, the objective function F to be minimized in the final data regression was also chosen as follows

$$F = \sum_{exp} \left| \frac{P^{exp} - P^{mod}}{P^{exp}} \right| \qquad (24)$$

where the P denotes either the CO_2 partial pressure (Bishnoi[2]; this work) or the total system pressure (Pérez-Salado Kamps[3]). The values for the obtained ionic interaction parameters W_{kl} are listed in Table 11 and further results of the data fit and modeling are listed in Table 12 and shown graphically in Figures 6–9.

As can be seen from Table 12, the average deviation between experimental and model pressure amounts to about 16%, which is good considering the experimental scatter.

Pérez-Salado Kamps et al.[3] used the Pitzer model to correlate their own CO_2 solubility in aqueous piperazine solutions. They report an average deviation of 4% between model and experiment. When applying their model to the data of Bishnoi,[2] a mean deviation of 22% between experiments and prediction was found. However, in their model, nine ionic interactions are present—all temperature dependent—giving a total of 18 fit parameters.

Besides the previously described "pressure–loading" curves, the presently developed VLE model is also useful for predicting speciation in loaded amine solutions. Information on the species distribution is indispensable when trying to predict acid gas absorption rates into (partially) loaded solutions, given that rigorous mass-transfer models require the exact bulk composition of the liquid phase.[33] Figure 10 shows a typical speciation plot of the PZ–H_2O–CO_2 system at 313 K.

As one can see from Figure 10, the contribution of the piperazine dicarbamate is never dominant, indicating that the theoretical chemical loading of 2 mol CO_2 per mol piperazine is never reached. At lower CO_2 loadings, both piperazine carbamate and protonated carbamate are present in the solution. On increasing loading (>0.5), however, the former is gradually converted to the latter, which can easily be explained by the accompanying decrease in pH of the solution. Similar speciation results were also reported by Bishnoi and Rochelle[2] and Pérez-Salado Kamps et al.[3]

The ability to predict speciation implies that the current model can also predict certain physical properties such as pH and (ionic) conductivity. Kaganoi[34] measured both pH and conductivity in loaded 0.6 M aqueous piperazine solutions. Those experimental data were extracted from the graphical representations in the paper by Bishnoi and Rochelle[2] and compared to predictions of the model presented in this work. Because the model does not include the H_3O^+ ion, pH values have been deduced from the OH^- ions present in the model. Results are shown in Figures 11 and 12.

Both Figure 11 and 12 show that the presently developed model is able to predict both pH and ionic conductivity reasonably well. Only at low loadings, however, does there seem to be a (consistent) discrepancy between the predicted and

Table 11. Ionic Interaction Coefficients W_{k1} Found in the Regression of the Experimental Database

W_{k1}	(10^3 m^3 mol^{-1})
PZH^+–H_2O	0.169
PZH^+–PZ	0.437
PZH^+–CO_2	0.074
PZH^+–$^+HPZCOO^-$	0.234
PZH^+–HCO_3^-	−0.023
PZH^+–$PZCOO^-$	−0.024
PZH^+–$PZ(COO^-)_2$	−0.202

Table 12. Experimental Database Used in the Data Fit and the Resulting Deviations with the Model

Source	[PZ]	Temperatures (K)	Loading Range (mol CO_2/mol PZ)	N*	AAD** (%)
This work	0.2 M	298, 313, 343	0.47–1.23	21	16.4
	0.6 M	298, 313, 343	0.36–1.08	30	19.9
Bishnoi[2]	0.6 M	313, 343	0.16–0.96	17	16.4
Pérez-Salado Kamps[3]	2.0 m	313, 333, 353, 373, 393	0.54–1.64	48	12.4
	4.0 m	333, 353, 373, 393	0.50–1.36	37	15.6
Total				153	15.7

* Number of data points used in the fitting procedure.
**AAD, average absolute deviation.

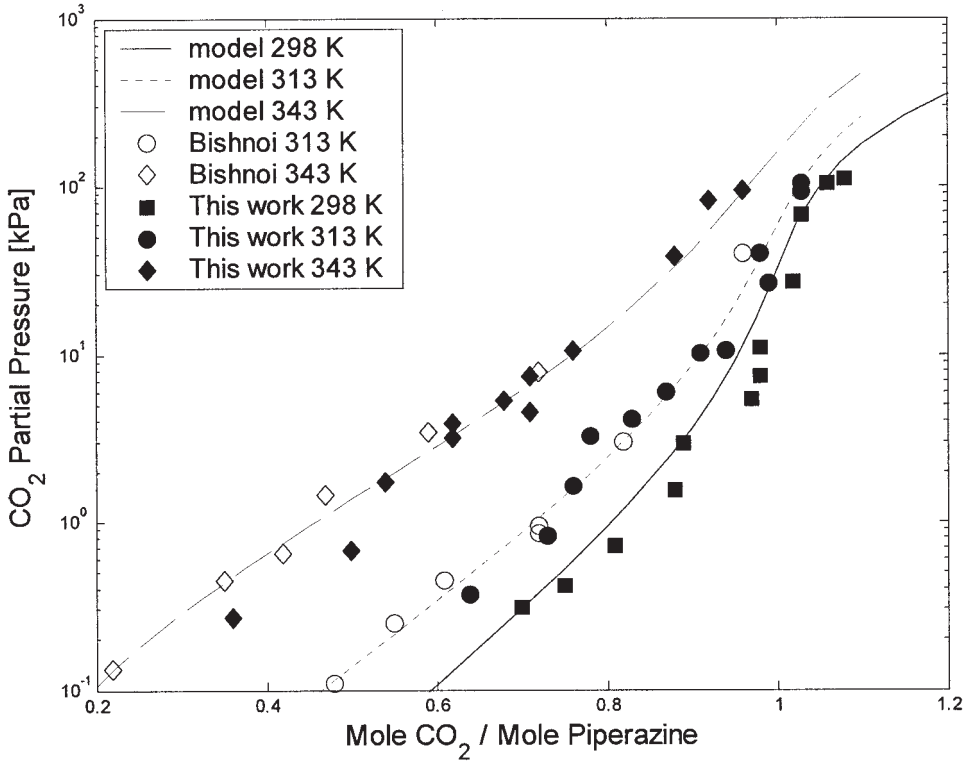

Figure 6. Representation of CO_2 solubility at various temperatures in the case of 0.6 M PZ solution.

measured pH. This might be caused by the binary parameters describing the piperazine–water interaction: Chang et al.[35] state that at low loadings, representation of acid gas solubility is sensitive to the binary amine–water interaction coefficients.

Conclusions

Removal of acid gases is usually achieved by absorption in solvents consisting of aqueous amine solutions. One very promising solvent is a blend of piperazine (PZ) and *N*-methyldiethanolamine (MDEA) solution in water (the so-called activated MDEA solvent). Detailed design of absorption–desorption units using this amine blend requires a thermodynamically sound composition model, not only to calculate equilibrium partial pressures over a (partially) loaded solution, but also to predict component speciation in the liquid bulk.

The present work adds new experimental data on the ternary subsystem PZ–H_2O–CO_2 at different concentrations and temperatures. The electrolyte equation of state (EoS), as originally proposed by Fürst and Renon,[13] has been used to correlate these and other available experimental data on the same system.

The final model contains a total of seven ionic parameters to be adjusted to an experimental database of 153 data points. The model was found to be able to predict CO_2 pressures with an average deviation of about 16% from experimental data.

Even though modeling results are satisfactory, some aspects of the currently presented EoS model can be further improved. Binary parameters on the piperazine-water system have been estimated using the UNIFAC method since no experimental data are available. No difficulties have been encountered in the present situation because it is known that the amine–H_2O interaction parameters in acid gas models are important in the low loading range.[35] As the current experimental database does not contain any data in the low loading range, the use of the UNIFAC method for the determination of the binary interactions of PZ with water seems acceptable. However, to obtain more precise values for these interaction coefficients, it is obvious that new, additional experimental data are needed.

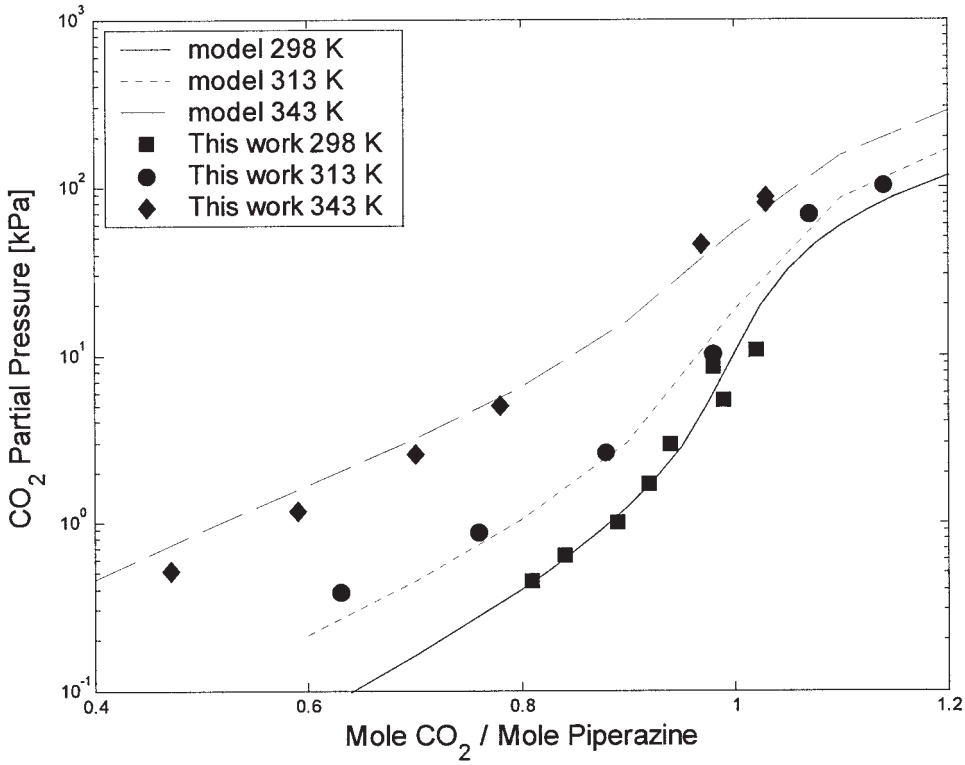

Figure 7. Representation of CO_2 solubility at various temperatures in the case of 0.2 M PZ solution.

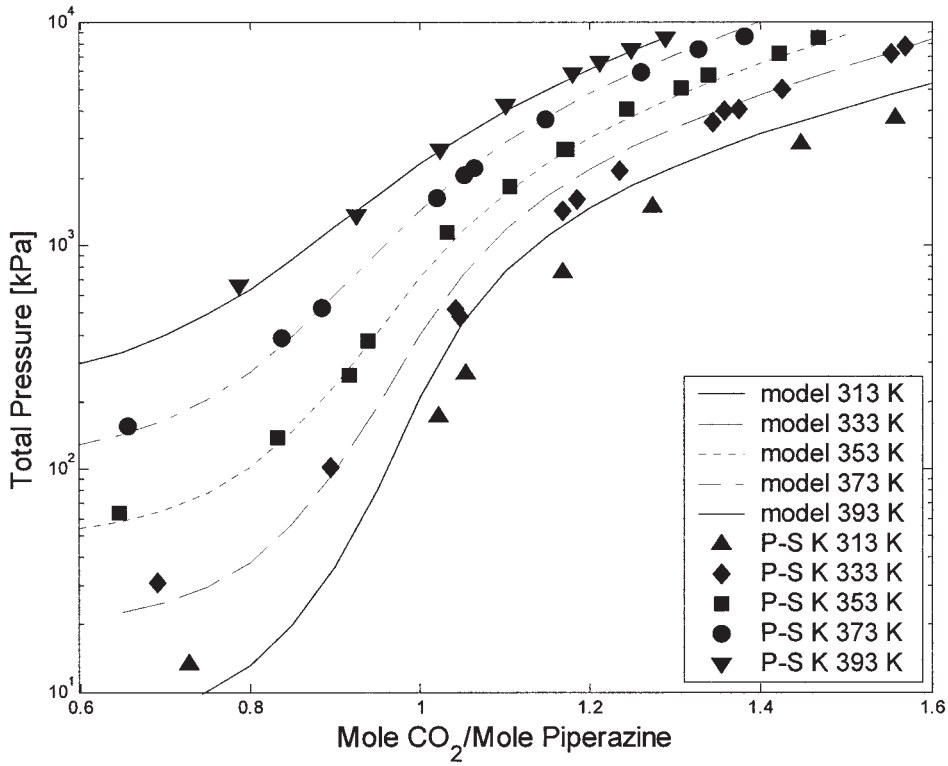

Figure 8. Representation of CO_2 solubility at various temperatures in the case of 2.0 m PZ solution.

P-S K denotes Pérez-Salado Kamps et al.[3]

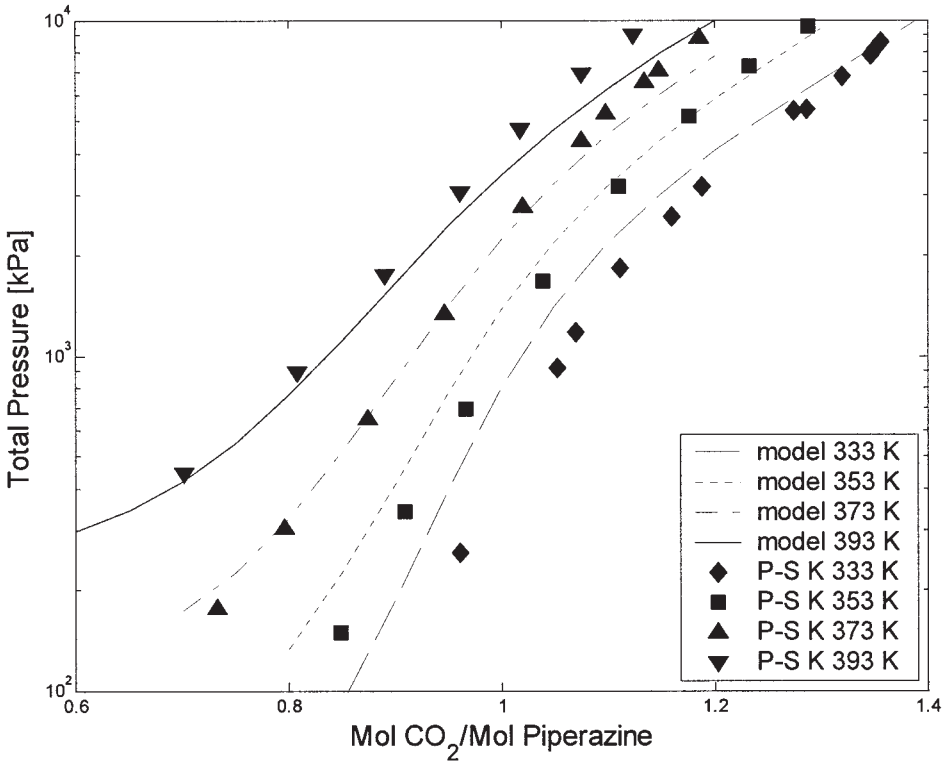

Figure 9. Representation of CO_2 solubility at various temperatures in the case of 4.0 m PZ solution.

P-S K denotes Pérez-Salado Kamps et al.[3]

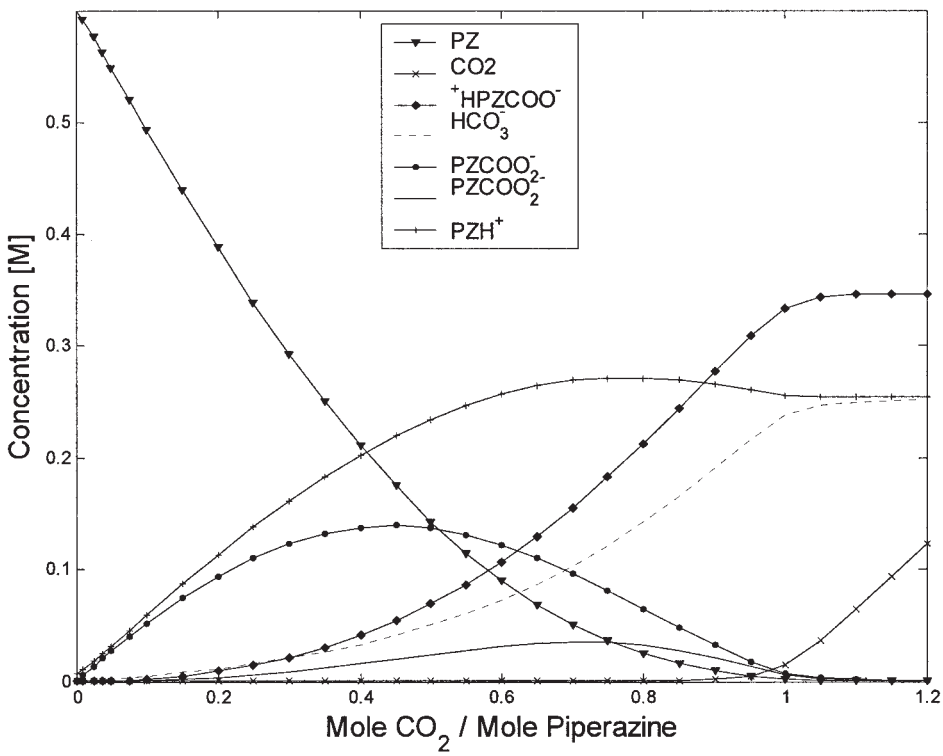

Figure 10. Predicted speciation of a 0.6 M PZ solution at 40°C.

It must be noted that points are not experimental data but results obtained by simulations, added for clarity.

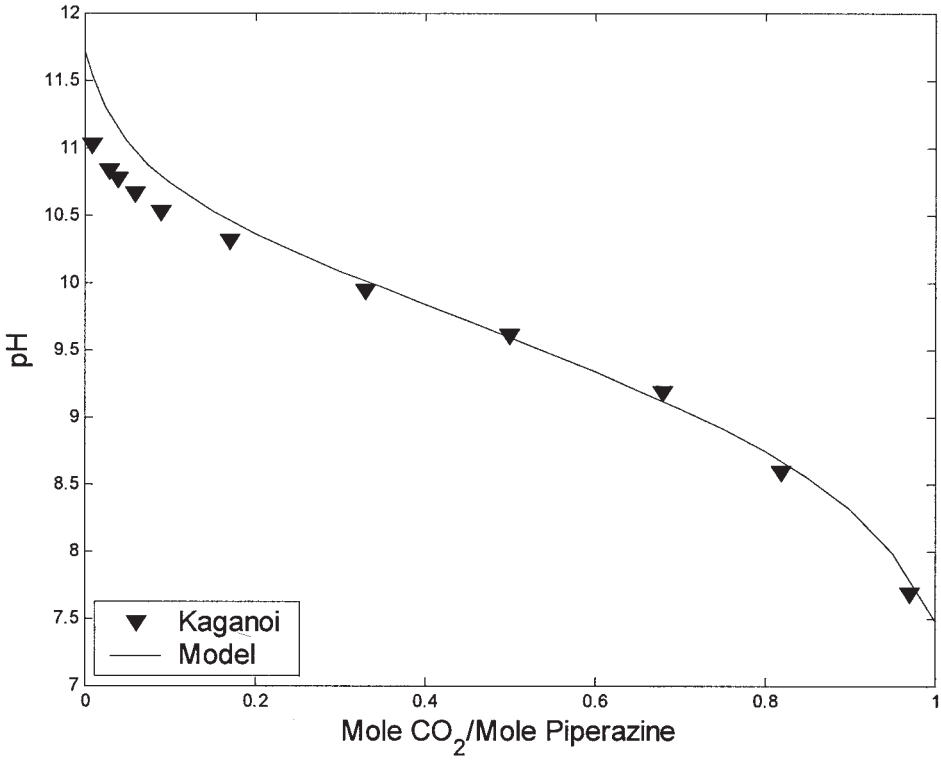

Figure 11. Comparison between experimental[2,34] and predicted pH of 0.6 M PZ solution loaded with CO_2.

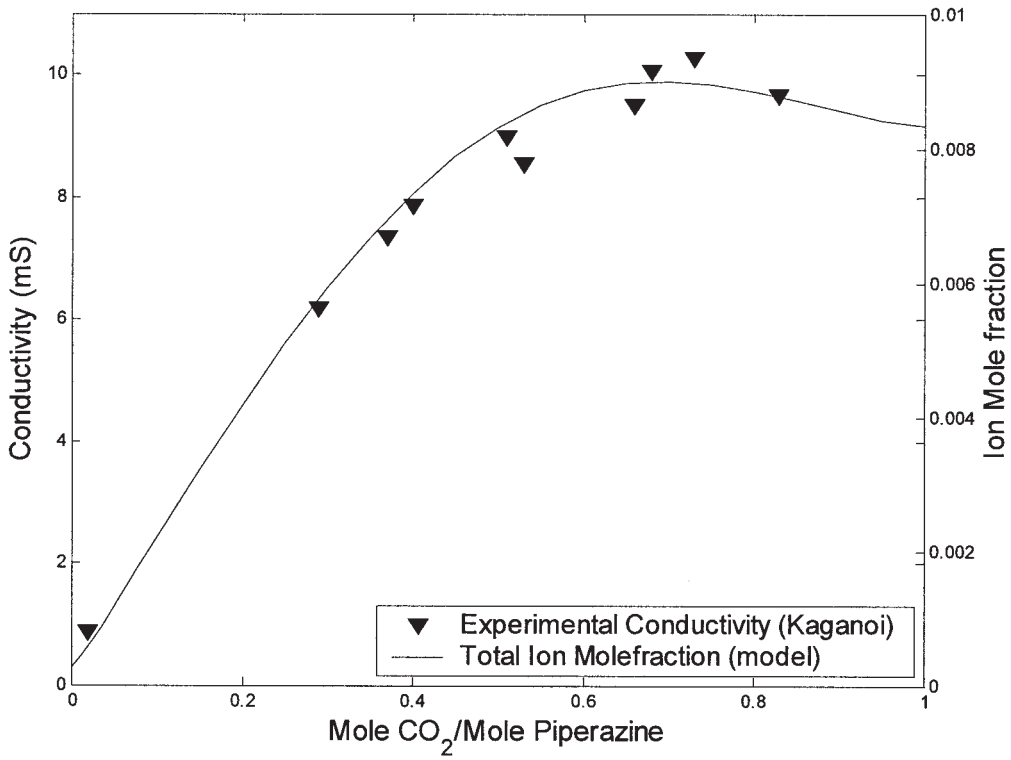

Figure 12. Measured[2,34] and predicted ionic conductivity in a 0.6 M PZ solution loaded with CO_2.

The results of the present work makes the extension of the EoS model toward the quaternary system water–methyldiethanolamine–piperazine–carbon dioxide possible.

Acknowledgments

The authors gratefully acknowledge Shell Global Solutions International BV for their financial support. Also, H. F. G. Moed is acknowledged for the construction of both experimental setups.

Notation

A = Helmholtz energy, J
A^{SR} = attraction parameter, J mol^{-1}
b = covolume, m^3 mol^{-1}
C = coefficients for equilibrium constant
D = dielectric constant
e = electron charge, C
f = fugacity, Pa
g_{mn} = interaction parameter in mixing rule, J m^{-3}
k_{mix} = binary interaction parameter in Eq. 20
K = equilibrium constant
m = molality, mol kg^{-1} water
M = molarity, mol L^{-1}
n = mole number, mol
N_A = Avogadro's constant, mol^{-1}
P = pressure, Pa
p_1, p_2, p_3 = polarity parameters
R = gas constant, J mol^{-1} K^{-1}
T = temperature, K
V = (molar) volume, m^3
W = electrolyte interaction parameter, m^3 mol^{-1}
x = liquid mole fraction
y = vapor mole fraction
Z = charge

Greek letters

α = (1) binary nonrandomness parameter; (2) correction factor for attraction parameter A^{SR}
α_{LR} = long range parameter in Eq. 14, m
γ = activity coefficient
Γ = shielding parameter, m^{-1}
ε_0 = vacuum electric permittivity, C^2 J^{-1} m^{-1}
ε_3 = packing factor
λ = ionic parameter in electrolyte EoS
ν = stoicheometric coefficient
σ = ionic/molecular diameter, m
σ^C, σ^P = solvated diameter, Å
τ = mixing rule parameter
φ = fugacity coefficient
Φ = osmotic coefficient
ω = acentric factor

Subscripts and superscripts

∞ = infinite dilution
a = anion
c = cation
C = critical
ion = ions/ionic
k, l = ionic or molecular
L = liquid phase
LR = long range
m, n, n' = molecular
mix = mixture
R = reduced/residual
RF = repulsive forces
S = solvent
SR = short range
V = vapor phase
Z = compressibility factor

Literature Cited

1. Kohl AL, Nielsen RB. *Gas Purification*. 5th Edition. Houston, TX: Gulf Publishing; 1997.
2. Bishnoi S, Rochelle GT. Absorption of carbon dioxide into aqueous piperazine: Reaction kinetics, mass transfer and solubility. *Chem Eng Sci*. 1999;55:5531-5543.
3. Pérez-Salado Kamps A, Xia J, Maurer G. Solubility of CO_2 in (H_2O + piperazine) and in (H_2O + MDEA + piperazine). *AIChE J*. 2003;49:2662-2670.
4. Aroua MK, Mohd Salleh R. Solubility of CO_2 in aqueous piperazine and its modelling using the Kent–Eisenberg approach. *Chem Eng Technol*. 2003;27:65-70.
5. Kent RL, Eisenberg B. Better data for amine treating. *Hydrocarb Process*. 1976;55:87.
6. Austgen DM, Rochelle GT, Peng X, Chen CC. Model of vapor–liquid equilibria for aqueous acid gas–alkanolamine systems using the electrolyte–NRTL equation. *Ind Eng Chem Res*. 1989;28:1060-1073.
7. Li YG, Mather AE. Correlation and prediction of the solubility of carbon dioxide in a mixed alkanolamine solution. *Ind Eng Chem Res*. 1994;33:2006-2015.
8. Fürst W, Planche H. Modélisation de la thermodynamique de l'extraction des gaz acides par les amines. *Entropie*. 1997;202/203:31-35.
9. Kuranov G, Rumpf B, Maurer G, Smirnova N. VLE modelling for aqueous systems containing methyldiethanolamine, carbon dioxide and hydrogen sulfide. *Fluid Phase Equilib*. 1997;136:147-162.
10. Chunxi L, Fürst W. Representation of CO_2 and H_2S solubility in aqueous MDEA solutions using an electrolyte equation of state. *Chem Eng Sci*. 2000;55:2975-2988.
11. Vallée G, Mougin P, Jullian S, Fürst W. Representation of CO_2 and H_2S absorption by aqueous solutions of diethanolamine using an electrolyte equation of state. *Ind Eng Chem Res*. 1999;38:3473-3480.
12. Solbraa E. *Equilibrium and Non-Equilibrium Thermodynamics of Natural Gas Processing*. PhD Thesis. Trondheim, Norway: Norwegian University of Science and Technology; 2002.
13. Fürst W, Renon H. Representation of excess properties of electrolyte solutions using a new equation of state. *AIChE J*. 1993;39:335-343.
14. Kumar PS, Hogendoorn JA, Timmer SJ, Feron PHM, Versteeg GF. Equilibrium solubility of CO_2 in aqueous potassium taurate solutions: Part 2. Experimental VLE data and model. *Ind Eng Chem Res*. 2003;42:2841-2852.
15. Blauwhoff PMM, Versteeg GF, Van Swaaij WPM. A study on the reaction between CO_2 and alkanolamines in aqueous solutions. *Chem Eng Sci*. 1984;39:207-255.
16. Ermatchkov V, Pérez-Salado Kamps A, Maurer G. Chemical equilibrium constants for the formation of carbamates in (carbon dioxide + piperazine + water) from ^{1}H-NMR-spectroscopy. *J Chem Thermodyn*. 2002;35:1277-1289.
17. Posey ML, Rochelle GT. A thermodynamic model of methyldiethanolamine–CO_2–H_2S–water. *Ind Eng Chem Res*. 1997;36:3944-3953.
18. Hetzer HB, Robinson RA, Bates RG. Dissociation constants of piperazinium ion and related thermodynamic quantities from 0 to 50°C. *J Phys Chem*. 1967;72:2081-2086.
19. Huron MJ, Vidal J. New mixing rules in simple equations of state for representing vapour–liquid equilibria of strongly non-ideal mixtures. *Fluid Phase Equilib*. 1979;3:255-271.
20. Schwartzentruber J, Renon H. Development of a new cubic equation of state for phase equilibrium calculations. *Fluid Phase Equilib*. 1989;52:127-134.
21. Ball FX, Planche H, Fürst W, Renon H. Representation of deviation from ideality in concentrated aqueous solutions of electrolytes using a mean spherical approximation molecular model. *AIChE J*. 1985;31:1233-1240.
22. Pottel R. *Water, A Comprehensive Treatise*. Vol. 3. New York, NY: Plenum Press; 1973.
23. Poling BE, Prausnitz JM, O'Connell JP. *The Properties of Gases and Liquids*. Fifth Edition. Boston: MA: McGraw-Hill; 2001.
24. Steele WV, Chirico RD, Knipmeyer SE, Nguyen A, Smith NK. Thermodynamic properties and ideal-gas enthalpies of formation for dicyclohexyl sulfide, diethylenetriamine, di-*n*-octyl sulfide, dimethyl carbonate, piperazine, hexachloroprop-1-ene, tetrakis(dimethylamino)ethylene, *N*,*N*′-bis-(2-hydroxyethyl)ethylenediamine, and 1,2,4-triazolo[1,5-*a*]pyrimidine. *J Chem Eng Data*. 1997;42:1037-1052.

25. Lide DR. *CRC Handbook of Chemistry and Physics*. 75th Edition. Boca Raton, FL: CRC Press; 1994.
26. *Ullmann's Encyclopedia of Industrial Chemistry*. 5th Edition, Vol. A2. Weinheim, Germany: VCH; 1994.
27. Simmrock KH, Janowsky R, Ohnsorge A. *Critical Data of Pure Substances—Chemistry Data Series*. Vol. 2, Part 1. Frankfurt am Main, Germany: DECHEMA; 1986.
28. Akhadov YY. *Dielectric Properties of Binary Solutions*. Oxford, UK: Pergamon Press; 1981.
29. Bishnoi S, Rochelle GT. Thermodynamics of piperazine/methyldiethanolamine/water/carbon dioxide. *Ind Eng Chem Res*. 2002;41:604-612.
30. Houghton G, McLean AM, Ritchie PD. Compressibility, fugacity and water solubility of carbon dioxide. *Chem Eng Sci*. 1957;6:184-185.
31. Zuo YX, Fürst W. Prediction of vapor pressure for nonaqueous electrolyte solutions using an electrolyte equation of state. *Fluid Phase Equilib*. 1997;138:87-104.
32. Robinson, RA, Stokes RH. *Electrolyte Solutions: The Measurement and Interpretation of Conductance, Chemical Potential and Diffusion in Solutions of Simple Electrolytes*. London: Butterworths Scientific; 1959.
33. Versteeg GF, Van Swaaij WPM. On the kinetics between CO_2 and alkanolamines both in aqueous and non-aqueous solutions—I. Primary and secondary amines. *Chem Eng Sci*. 1988;43:573-585.
34. Kaganoi S. *Carbon Dioxide Absorption in Methyldiethanolamine with Piperazine or Diethanolamine*. MS Thesis. Austin, TX: University of Texas; 1997.
35. Chang HT, Posey ML, Rochelle GT. Thermodynamics of alkanolamine–water solutions from freezing point measurement. *Ind Eng Chem Res*. 1993;32:2324-2335.

Manuscript received Aug. 30, 2004, and revision received Nov. 9, 2004.